Annals of Botany **117**: 599–606, 2016
doi:10.1093/aob/mcw007, available online at www.aob.oxfordjournals.org

ANNALS OF BOTANY
Founded 1887

The gelatinous extracellular matrix facilitates transport studies in kelp: visualization of pressure-induced flow reversal across sieve plates

Jan Knoblauch, Winfried S. Peters[†] and Michael Knoblauch*

School of Biological Sciences, Washington State University, PO Box 644236, Pullman, WA 99164, USA
**For correspondence. E-mail knoblauch@wsu.edu*
[†]*On sabbatical leave from: Indiana/Purdue University Fort Wayne, 2101 East Coliseum Boulevard, Fort Wayne, IN 46805, USA.*

Received: 3 October 2015 Returned for revision: 7 November 2015 Accepted: 8 December 2015 Published electronically: 29 February 2016

• **Background and Aims** In vascular plants, important questions regarding phloem function remain unanswered due to problems with invasive experimental procedures in this highly sensitive tissue. Certain brown algae (kelps; Laminariales) also possess sieve tubes for photoassimilate transport, but these are embedded in large volumes of a gelatinous extracellular matrix which isolates them from neighbouring cells. Therefore, we hypothesized that kelp sieve tubes might tolerate invasive experimentation better than their analogues in higher plants, and sought to establish *Nereocystis luetkeana* as an experimental system.
• **Methods** The predominant localization of cellulose and the gelatinous extracellular matrix in *N. luetkeana* was verified using specific fluorescent markers and confocal laser scanning microscopy. Sieve tubes in intact specimens were loaded with fluorescent dyes, either passively (carboxyfluorescein diacetate; CFDA) or by microinjection (rhodamine B), and the movement of the dyes was monitored by fluorescence microscopy.
• **Key Results** Application of CFDA demonstrated source to sink bulk flow in *N. luetkeana* sieve tubes, and revealed the complexity of sieve tube structure, with branches, junctions and lateral connections. Microinjection into sieve elements proved comparatively easy. Pulsed rhodamine B injection enabled the determination of flow velocity in individual sieve elements, and the direct visualization of pressure-induced reversals of flow direction across sieve plates.
• **Conclusions** The reversal of flow direction across sieve plates by pressurizing the downstream sieve element conclusively demonstrates that a critical requirement of the Münch theory is satisfied in kelp; no such evidence exists for tracheophytes. Because of the high tolerance of its sieve elements to experimental manipulation, *N. luetkeana* is a promising alternative to vascular plants for studying the fluid mechanics of sieve tube networks.

Key words: Alginate, brown algae, long-distance transport, microinjection, Münch flow, *Nereocystis luetkeana*, Laminariales, Phaeophyceae, phloem, photoassimilate transport, sieve plate, sieve tube.

INTRODUCTION

In higher plants, some organs fix more carbon through photosynthesis than they require themselves. The surplus is exported to organs that need more photosynthates than they produce, or is released to the environment (Savage *et al*., 2015). The routes for this source to sink transport of photoassimilates are the sieve tubes of the phloem, which form a symplasmic network of tubular cells called sieve elements (Esau, 1969; Evert, 1982). Symplasmic connectivity of the transport path is achieved through large pores in the cross-walls between sieve elements. These perforated walls, the so-called sieve plates, are the characteristic anatomical feature of sieve tubes (Esau, 1969; Mullendore *et al*., 2010; Jensen *et al*., 2012). Today, the commonly accepted transport mechanism is Münch flow, i.e. symplasmic bulk flow that is driven by osmotically generated pressure gradients along the translocation pathway. However, it has been argued that the wide acceptance of Ernst Münch's model (Münch, 1930) rests on its undoubted plausibility rather than on unequivocal experimental support (Thompson, 2006; Knoblauch and Peters, 2010; Knoblauch and Oparka, 2012). Experimental tests of predictions derived from Münch's model are complicated mainly by two factors. First, phloem transport is a systemic phenomenon that cannot be studied in isolated cells. Secondly, the extreme sensitivity of sieve elements has prevented an understanding of the structure of these cells in the functional state for over 150 years, and is hampering experimental manipulations of functional phloem tissue (e.g. Fischer, 1885; Johnson *et al*., 1976; Spanner, 1978; Ehlers *et al*., 2000; Knoblauch *et al*., 2014).

Brown algae (Phaeophyceae; Heterokonta/Stramenopila) evolved multicellularity independently of land plants (Archibald, 2012; Katz, 2012). Nonetheless, brown algae of the order Laminariales, the kelps, possess sieve elements for the long-distance transport of photoassimilates that are strikingly similar to those found in land plants (Buggeln, 1983; Schmitz, 1990; Raven, 2003). In both cases, translocation appears to be achieved through cytoplasmic bulk flow in symplasmically continuous arrays of sieve elements, but only in vascular plants has this been directly visualized on the cellular level by the movement of fluorescent dyes (Knoblauch and van Bel, 1998). The convergent evolution of sieve tube-based transport systems is not surprising, since cytoplasmic mass flow will necessarily occur in walled cells if intracellular or extracellular gradients in osmolarity exist. Therefore, the evolution of symplasmic networks in which

Münch flow operates is readily explained as an optimization of ubiquitous biophysical processes in walled cells (Knoblauch and Peters, 2013; see also Abadeh and Lew, 2013).

However, there are significant structural differences between the sieve tube networks in vascular plants and kelps. In contrast to the situation in land plants, the sieve elements of kelps are not in close contact with neighbouring cells. Since there are no analogues of companion cells or phloem parenchyma in kelp (Schmitz, 1990), kelp sieve tubes are comparatively easily identified and observed under the microscope. Kelp blades and stipes usually consist of a central medulla covered by cortex tissue and a photosynthetically active dermal layer called the meristoderm (Oltmanns, 1922; Nicholson, 1976; Schmitz and Srivastata, 1976). The sieve elements are found in the medulla, where they are embedded in a gelatinous extracellular matrix that occupies significant proportions of the medullar volume. As in higher plants, cellulose is the main component of the immediate cell wall that encloses the cells. The gelatinous extracellular matrix, on the other hand, consists mostly of alginates which are polymers of guluronic and mannuronic acid monomers at varying proportions (Percival, 1979; Percival and McDowell, 1981; Deniaud-Bouët *et al*., 2014). Alginates form elastic, swellable gels not unlike the familiar agar media (Kloareg and Quatrano, 1988; Draget *et al*., 1997), providing kelp sieve elements with a very different biomechanic microenvironment from that which their analogues experience in vascular plants.

An essential requirement of Münch's model is the openness of sieve tubes and sieve plates for pressure-driven bulk flow. If the model is valid, locally imposed pressure gradients will (re)direct flow patterns, which could be visualized by fluorescent dyes. On various occasions, we had attempted to create such local pressure gradients by microinjection techniques in angiosperm sieve tubes. We failed consistently to revert flow direction across sieve plates due to methodological difficulties. Studies of this kind are complicated, as Weatherley and Johnson (1968) stated in their classical review, by 'the fact that sieve tubes ... are dispersed among other cells of different function and are easily damaged'. For precisely these reasons, kelp sieve elements should lend themselves to invasive manipulations such as microinjection experiments: the absence of neighbouring cells should enable the approach to an individual sieve element without inducing injury responses in the vicinity, and the gelatinous extracellular matrix should provide an elastic bearing to stabilize impalements and prevent leakage.

Bull kelp (*Nereocystis luetkeana*) is an ecologically important species of the north Pacific (Springer *et al*., 2010). All photosynthesizing blades of an individual emerge from a single bulbous float and elongate by means of growth zones at their bases (Kain, 1987). Each basal growth zone is a sink that imports photoassimilates via sieve tubes in the blade medulla (Nicholson, 1970, 1976; Schmitz and Srivastata, 1976) from the distal, mature portion of its blade that serves as a source (Nicholson and Briggs, 1972; Schmitz and Lobban, 1976). Here we report the establishment of *N. luetkeana* as an experimental system for the study of sieve tube fluid mechanics. In the process, we visualized mass flow in individual sieve tubes as well as in lateral connections between tubes, demonstrated the feasibility of high-resolution flow velocity measurements in individual tubes, and finally induced the temporary reversal of flow direction across sieve plates by pressure-injection of dye solution into translocating tubes.

MATERIALS AND METHODS

Experimental organisms

Complete *Nereocystis luetkeana* [(K. Mertens) Postels and Ruprecht 1840, Laminariaceae] growing in the wild were collected by scuba divers in Barkley Sound close to Bamfield Marine Science Station, Bamfield, BC, Canada (48 °50'N, 125 °08'W). Intact thalli were kept in running seawater tanks at the station, and experiments were performed within 24 h of collection.

Microscopy of functional sieve elements in intact thalli

To observe functional sieve tubes in otherwise intact specimens, small squares (5 × 5 mm) of the meristoderm and cortex were removed by paradermal hand sections with razor blades to expose the medulla without sieve element injury. Parts of blades that were exposed to air were wrapped in paper towels and kept moist with fresh seawater. Blades were mounted on custom-built plexiglas stages to provide sufficient support and prevent tissue movement during observation. The observation area was submerged in seawater and examined with dip-in lenses not corrected for cover slips (Leica HCX-PlanApo U-V-I) using a Leica DM 2500 fluorescence microscope (Leica, Wetzlar, Germany). Micrographs and time series were recorded using a Leica DFC-300 cooled CCD camera mounted on the microscope and connected to a laptop computer.

For CFDA (carboxyfluorescein diacetate) translocation studies, 25 mg of CFDA (Molecular Probes, Novato, CA, USA) were dissolved in 1 mL of acetone; 10 µL of this stock solution were added to 1 mL of seawater and injected into the medulla with a syringe. CFDA readily enters cells where it is cleaved to form CF (carboxyfluorescein), which is non-permeant and remains within the cytoplasm. Fluorescence was observed with a Leica I3 filter block.

For dye injection into individual sieve elements, microcapillaries were pulled from borosilicate glass tubes of 1 mm outer and 0·5 mm inner diameter (Harvard Apparatus, Holliston, MA, USA) with a Sutter Instruments laser puller model P-2000 (Sutter Instruments, Novato, CA, USA). Capillary tips were backfilled with 0·5 µL of rhodamine B (Sigma-Aldrich, St. Louis, MO, USA), a membrane-impermeant fluorescent dye, and the remainder of the capillary was filled with 50 cSt silicone oil to exclude air. Injection experiments were performed with a custom-built cell pressure system attached to the Leica DM 2500 microscope. Fluorescence was observed with a Leica N2.1 filter block.

Microscopy of fixed tissue samples

Nereocystis blade excisates were stored in 70 % ethanol at −20 °C. For histological studies, pieces 2 mm thick were microwave-fixed in 2 % glutaraldehyde, 2 % paraformaldehyde, 0·1 M cacodylate buffer, 2 mM calcium chloride and 10 mM ruthenium red for 2 min 30 s on ice. The material was

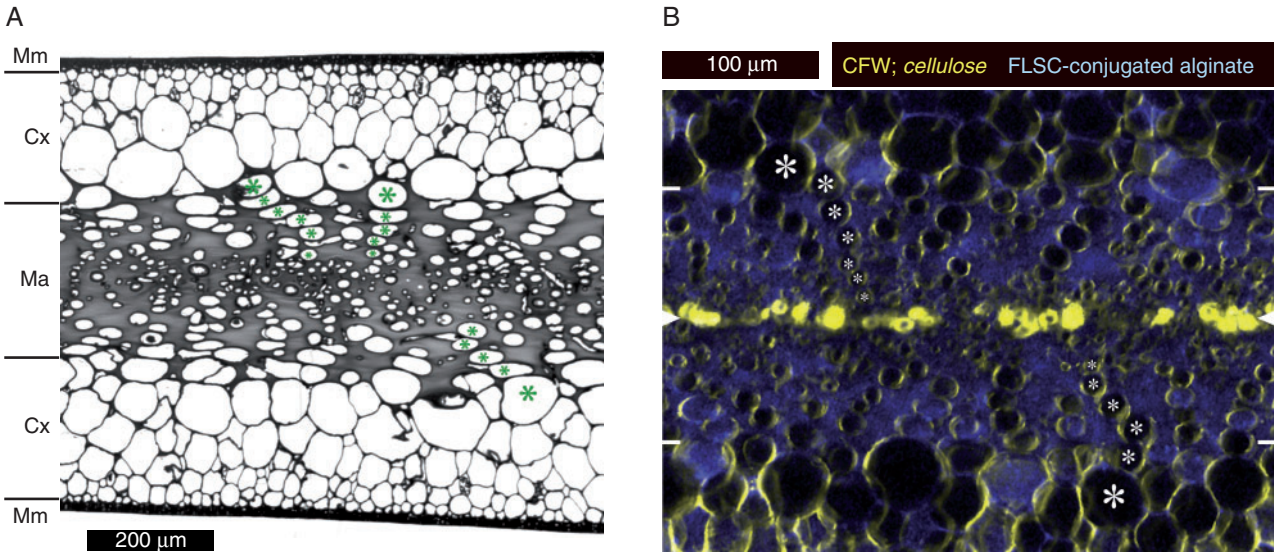

FIG. 1. Anatomy of blades of *Nereocystis luetkeana*. (A) Conventional bright-field micrograph of a cross-section of a toluidine blue-stained segment embedded in Spurr's resin. The meristoderm (Mm), cortex (Cx) and medulla (Ma) are marked. The gelatinous extracellular matrix occupies a large part of the medulla and shows as a solid grey mass. Rows of longitudinally oriented tubular cells extend from the inner cortex into the medulla; examples are marked (*). Sieve elements are usually found in the centre of the medulla, but cannot be identified unambiguously in cross-sections. (B) Double-fluorescence micrograph of a medulla cross-section (hand section); mid-plane and outer borders of the medulla are indicated by white arrowheads and white lines, respectively, at the edges of the image. Characteristic rows of cells are marked as above (*). Immediate cell walls exhibit high cellulose contents (calcofluor white, CFW; shown in yellow), while the gelatinous extracellular matrix fluoresces due to the integration of fluorescein (FLSC)-conjugated alginate (blue). Conspicuous cellulose accumulations in the mid-plane probably correspond to old, collapsed sieve elements.

washed twice in 2 mM cacodylate buffer with 2 mM calcium chloride, and then post-fixed in 2 % osmium tetroxide. Samples were stained overnight at 4 °C in 2 % uranyl acetate, 0·5 % ruthinium red and 0·5 % potassium permanganate, dehydrated in an ethanol series and embedded in Spurr's resin. Sections of 1 µm thickness were cut with a Leica Ultracut R ultramicrotome and stained with toluidine blue for 1 min at 60 °C. Images were taken with a Leica DFC 300 camera attached to a Leica DM 2500 microscope. The proportion of the volume of the medulla occupied by extracellular matrix was estimated from the area covered by extracellular material in the micrographs using ImageJ v1.48 (http://imagej.nih.gov/ij).

For localization studies of cellulose and alginate, blade material stored in 70 % ethanol was rehydrated in seawater. Calcofluor white solution (product # 6726; Eng Scientific Inc., Clifton, NJ, USA), a selective cellulose marker, was added to a final concentration of 0·1 %. Fluorescein-conjugated alginate was synthesized according to Vreeland and Laetsch (1989). The conjugate was dissolved in seawater to a final concentration of 0·01 %, and blade sections were exposed to the solution for 1 h. Calcofluor white was excited with a 405 nm diode laser and emission was passed through a 420–480 nm band pass filter, while fluorescein was excited at 488 nm and excitation was observed with a 510 nm long pass filter on a Zeiss 510 Meta confocal microscope.

Image processing

Micrograph acquisition was controlled with the Leica LAS V3.8 software, and the pixel size of the original micrographs was adjusted linearly as required for publication. All image manipulations (brightness and contrast adjustment, coloration and colour adjustments, thresholding) were applied equally to entire images and image series using Paint Shop Pro v.6 (JASC Software, now Corel; www.corel.com) and ImageJ v1.48 (http://imagej.nih.gov/ij). Time series of micrographs were processed to obtain videos using Quicktime Pro v.7.7.6 (www.apple.com/quicktime) and Animation Shop v.2.00 (JASC Software, now Corel; www.corel.com).

RESULTS

Blades of *Nereocystis luetkeana* consist of three clearly identifiable tissues. The central medulla is located between two layers of large-celled cortex, and this sandwich structure is enclosed in a sheath of small-celled meristoderm (Fig. 1A). The medulla is characterized by a high proportion of gelatinous extracellular matrix. We estimated the proportion of the volume of the medulla that was occupied by extracellular material to range between 67 and 82 %, based on quantifications of areas covered in six different cross-sections (not shown; the value is 73 % for the representative section in Fig. 1A). Large, longitudinally oriented tubular cells extended in conspicuous rows from the inner cortex towards the mid-plane of the blade, where sieve elements could be found (Fig. 1A; compare Nicholson, 1976). Double fluorescence staining using a specific cellulose marker (calcofluor white) and fluorescein-conjugated alginate, which forms complexes with native alginate *in situ*, confirmed the cellulose richness of the immediate cell wall and the high alginate contents of the gelatinous extracellular matrix (Fig. 1B).

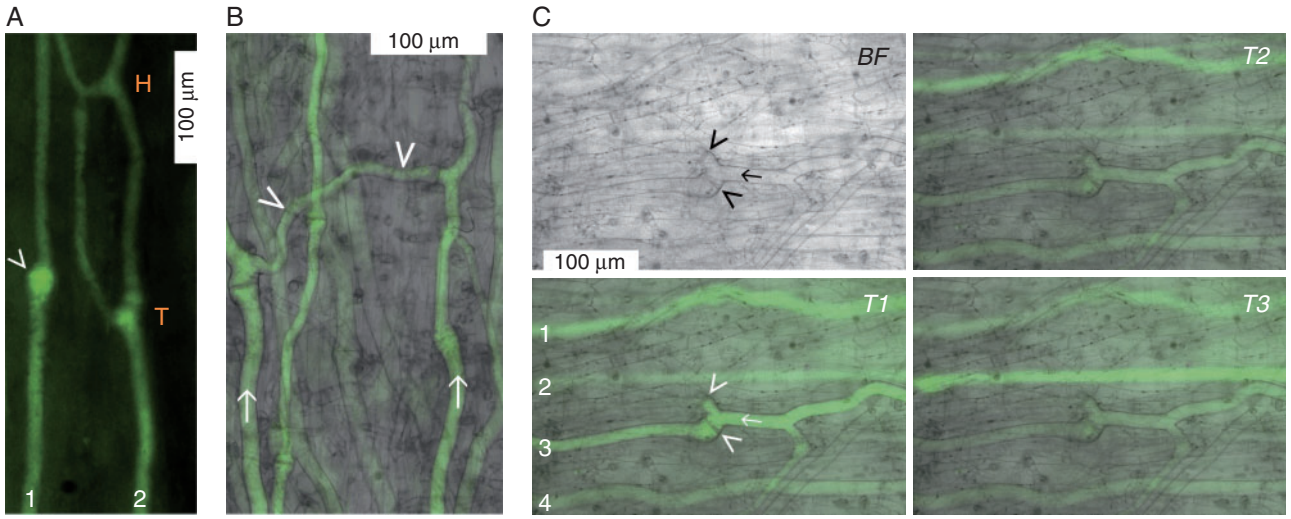

FIG. 2. Complexity of the sieve tube network in mature blades of *Nereocystis luetkeana*. (A) Translocating sieve tubes observed through a window of removed peripheral tissues. The long axis of the blade runs from the bottom of the image (source-ward) to the top (sink-ward). Shortly after injection of carboxyfluorescein diacetate (CFDA) into the medulla about 8 cm distal of the tissue shown, CF fluorescence appeared in the monitored region. Sieve tube 1 is unbranched and has a sieve plate in a bulbous distension (arrowhead), while sieve tube 2 is branched and shows a T as well as an H junction. (B) Two transporting sieve tubes (arrows) oriented more or less parallel to the long axis of the blade [bottom (source) to top (sink)] are connected laterally by a slightly thinner but also transporting tube (arrowheads). (C) The brightfield micrograph (BF; top left) is focused on the central part of a sieve tube (arrow) between two T junctions; the two branches of the downstream T junction have sieve plates at their bases (arrowheads). The blade axis runs right (source) to left (sink). Fluorescence micrographs taken with identical microscope settings at arbitrary times (T1, T2, T3) within 2 min after the appearance of the CF signal show independently fluctuating signal intensities in four sieve tubes (1–4). Only one branch of the downstream T junction of sieve tube 2 is transporting (T1).

Next, we attempted to verify that long-distance transport occurred in sieve tubes, which has not been directly demonstrated in live kelp to date. Intact specimens kept in tanks in the lab were used. We injected the fluorescent dye, CFDA, into the medulla of mature blade regions and monitored the appearance of CF fluorescence a few centimetres downstream (i.e. closer to the blade's base). Several minutes after injection, the signal reliably appeared in mature sieve elements in the monitored downstream regions. Immature sieve elements, identifiable by large numbers of vesicles (Schmitz and Srivastava, 1976), never fluoresced. Transporting sieve tubes exhibited structural complexity, with various combinations of T and H junctions (Fig. 2A), and lateral connections between parallel sieve tubes (Fig. 2B). Occasionally, some, but not all, branches of a junction were actively transporting (for an example, see Fig. 2C), suggestive of differential flow regulation within the network. The intensities of the fluorescence tended to fluctuate irregularly and independently in individual sieve tubes (Fig. 2C), indicating differential loading and/or transport rates. We concluded that flow velocities measured in individual tubes would probably vary widely.

To evaluate the hypothesized usefulness of the elastic gelatinous extracellular matrix in microinjection experiments, we injected a solution of rhodamine B, a membrane-impermeant fluorescent dye, into individual sieve elements of blades of intact specimens. In initial experiments, we injected the dye continuously and observed bulk movement along the tubes and across sieve plates (Fig. 3A). However, to overcome turgor, significant pressure has to be applied to inject the dye solution into a cell. Continuous injection requires continuous pressure application, which must be expected locally to distort the natural pressure gradients that drive sieve tube flow. The effects of these distortions could be minimized (or, hopefully, totally avoided) if flow velocities were determined after a pulsed application of injection pressure. Therefore, we determined flow velocities from the movement of dye pulses. We processed the obtained micrographs by setting a threshold to 12–15 %, depending on the contrast in the original images series, of the maximum intensity of the fluorescence signal. By measuring the progress of the dye front in the thresholded micrographs (as shown in Fig. 3B and Supplementary Data Video S1), we minimized the uncertainty that resulted from the subjective determination of the location of the dye front which blurred and widened over time due to the diffusion of the dye. Since this type of velocity measurement can be performed numerous times on the same sieve tube within a few seconds (see Video S1), it allows the determination of mean values and their variances for individual tubes over very short periods. Thus, the method can provide a measure of the variance due to measurement error (expressed as s.d. in Video S1) as opposed to the biological variance between individual tubes, between specimens or between measurements taken at different times in the same tube. In the eight sieve tubes of three thalli in which we tested our microinjection methodology, we found an apparently random distribution of flow velocities ranging from 0 to 124 µm s^{-1}. This corresponded to our above conclusion from CFDA application tests that flow rates in different segments of the sieve tube network might differ significantly. Obviously, more systematic investigations are needed to understand patterns of flow velocity and their regulation in the complex 3-D network of sieve tubes.

Dye injection into individual sieve tubes was a relatively simple procedure in *N. luetkeana* compared with the vascular plants we had used in previous studies. Impalements were

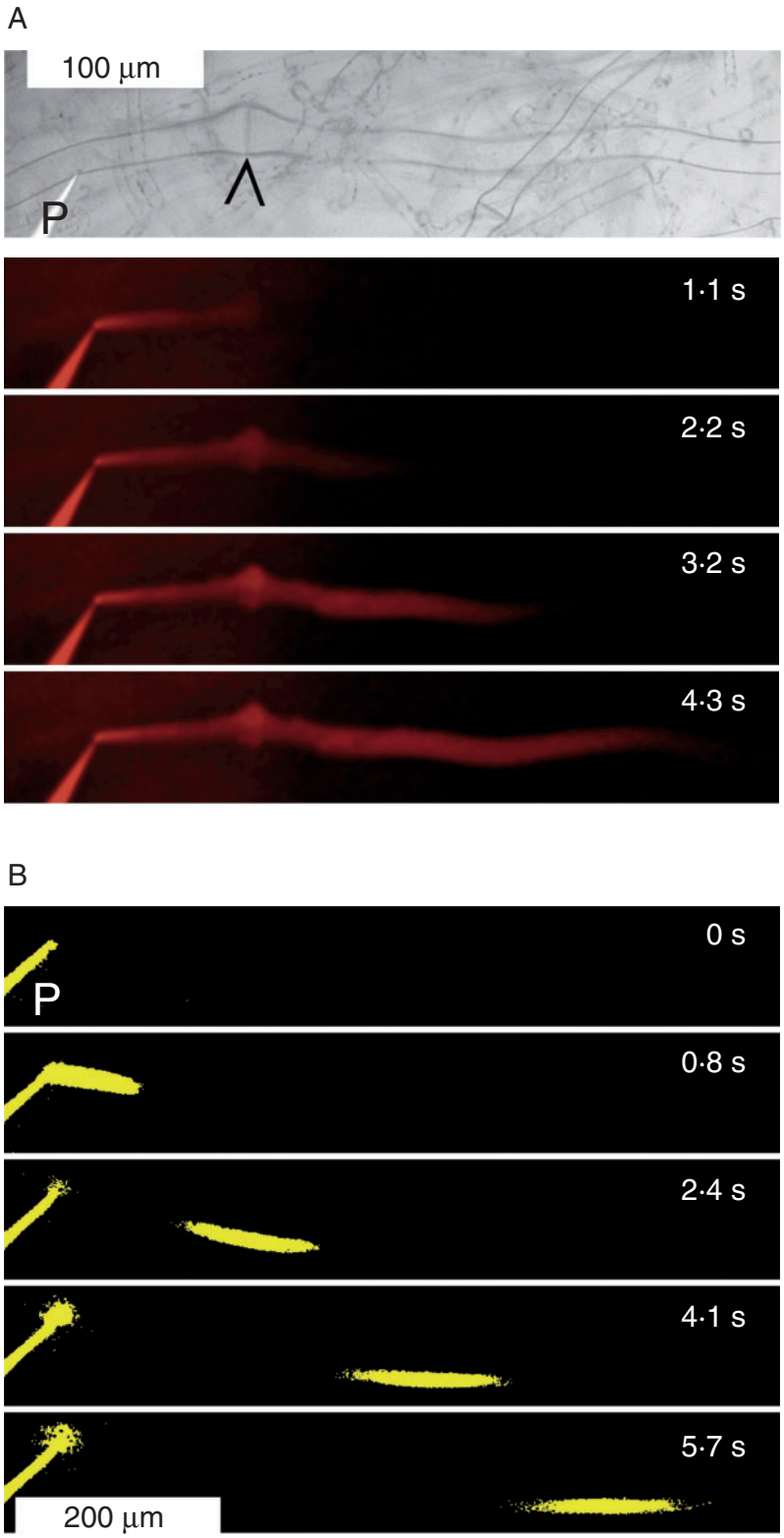

FIG. 3. Determination of flow velocity in individual sieve tubes of *Nereocystis luetkeana*. (A) The brightfield micrograph on top shows a sieve tube with sieve plate (arrowhead) and a micropipette (P) before insertion into the tube. The blade axis runs left (source) to right (sink). Four fluorescence micrographs of the same tube are shown below, taken at the indicated times after the start of continuous rhodamine B injection to visualize transport across the sieve plate and beyond. (B) Pulse injection of rhodamine B into a sieve tube; images show the fluorescence thresholded at 14 % of the maximum intensity in the original micrographs. At 0 s, only the pipette (P) is visible. Subsequent images show the dye pulse moving along the sieve tube. Flow velocity was determined from the movement of the dye front in such image series. As shown in Supplementary Data Video S1, the mean flow velocity in this particular experiment was 120 μm s^{-1}.

stable over several minutes (in some instances approaching the half hour mark) and leakage rarely occurred, as we had hoped. Consequently, we attempted to visualize pressure-driven reversals of flow across sieve plates. We placed micropipettes on the expected downstream side of sieve plates (Fig. 4A) and injected pulses (1·5 s) of rhodamine B solution. The resulting pressure waves drove small amounts of dye across the sieve plate into the upstream sieve element, from where the dye translocated back in the downstream direction immediately after the pressure pulse had ended (Fig. 4B; Supplementary Data Video S2). The experiment could be repeated several times in the same sieve tubes, which emphasized the stability of the impalements and spoke against any functionally significant damage in the manipulated tubes. The amount of dye that was driven across sieve plates in the reverse direction depended on the magnitude of the injection pressure applied (Fig. 4C). This fact was demonstrated by consecutive injections at stepwise increased pressure (Video S2), although the response time of the digital pressure gauge of our custom-built injection system was too long to enable the accurate quantification of pressure changes that occurred over 2 s or less.

DISCUSSION

Despite the structural similarity of tracheophyte and kelp sieve tubes, the involvement of the latter in long-distance photoassimilate transport had not been demonstrated unequivocally. Immature kelp sieve elements typically contain numerous vesicles, which disappear as the cell differentiates into a mature sieve tube member (Schmitz and Srivastava, 1976). Early studies in *Laminaria*, in which the translocation of radiolabeled photoassimilates was detected by histoautoradiography, had seemed to indicate translocation in young sieve elements that apparently were blocked by vesicles (Steinbiß and Schmitz, 1973). Consequently, Schmitz and Srivastava (1974) inferred that bulk flow was an unlikely transport mechanism in sieve tubes of kelps. This argument is resolved by the direct observation of bulk flow through the movement of fluorescent dyes in mature but not in immature sieve elements of *N. luetkeana* (Figs 2–4; Supplementary Data Videos S1 and S2).

The visualization of bulk flow in the sieve elements of angiosperms (Knoblauch and van Bel, 1998; Froelich *et al*., 2011) as well as kelp (this study) supports the idea that brown algae and green plants independently evolved similar machineries for the long-distance transport of photoassimilates. A precise, quantitative understanding of these machineries and the forces that drive them, however, is lacking, due to the sensitivity of the higher plant phloem on which research in the field is focused. Our observations in *N. luetkeana* suggest that kelp sieve tubes are a more tolerant experimental system than their higher plant equivalents, probably because kelp tubes are embedded in a mechanical buffer provided by the gelatinous extracellular matrix, and because transporting kelp sieve elements can be manipulated without wounding of cells in the immediate vicinity. The visual demonstration of pressure-induced, rapid reversals of transport direction across sieve plates (Fig. 4; Supplementary Data Video S2) establishes conclusive evidence that the sieve plate is traversable for pressure-driven bulk flow, a critical requirement of the Münch theory (Münch, 1930). No such direct demonstration is available from higher plants.

Previous estimates of photosynthate transport velocities in *N. luetkeana* were based on the bulk translocation of ^{14}C-labelled photoassimilates in whole blades of intact thalli. Two independent studies reported translocation velocities ranging from 11 to 18 cm h^{-1} (average 17 cm h^{-1}; Schmitz and Lobban, 1976) and from 20 to 50 cm h^{-1} (average 37 cm h^{-1}; Nicholson and Briggs, 1972). In these experiments, translocation was detected over periods of several hours and distances of several decimetres. In contrast, our pulsed dye injection experiments (Fig. 3B; see also Supplementary Data Video S1), which were conducted to establish the feasibility and usefulness of comparatively simple microinjection techniques in kelp sieve tubes, allowed for direct measurements of transport velocities in individual sieve tubes at sub-cellular spatial and sub-second temporal resolution. The direct observation of dye translocation in functional sieve tubes in intact kelp indicated maximum transport velocities of about 120 µm s^{-1} (43 cm h^{-1}). Maximum velocities in individual sieve tubes determined over micrometre distances (this study) have to be expected to be relatively high compared with velocity estimates based on radiolabel movements over decimetre distances in intact thalli (Nicholson and Briggs, 1972; Schmitz and Lobban, 1976) since sieve tubes usually are branched, curved, and slightly oblique with respect to the long axis of the blade, and thus are not generally aligned with the shortest possible distance between sources and sinks. Therefore, our results appear in good agreement with the earlier reports. On the other hand, our observations of apparently non-transporting tubes next to transporting tubes suggest complex, differentially regulated patterns of flow velocities in the 3-D sieve tube arrays. The future characterization of such patterns by established methods now appears possible in kelp but not necessarily in vascular plants, due to the differences in the sensitivity of the conducting tissues between the two taxa.

The phylogenetic distance between brown algae and flowering plants is as large as it can be between two clades of multicellular eukaryotes (Lane and Archibald, 2008). However, the explanatory power of functional models does not depend on phylogenetic relationships – after all, Münch's idea became widely accepted not because he could experimentally demonstrate his proposed mechanism to operate in living plants, but because his artificial models – interconnected osmotic cells that he assembled in the classroom – possessed a striking, intuitive plausibility (for a discussion, see Knoblauch and Peters, 2010). At this time, available evidence supports the notion that fundamental mechanisms of the long-distance transport of photoassimilates are similar in kelps and vascular plants (Behnke and Sjolund, 1990; Raven, 2003; Knoblauch and Peters, 2013, and references therein). Understanding the biophysics underlying the differential regulation of flow patterns in the 3-D sieve tube networks of kelp will certainly not answer all questions about the phloem in higher plants. However, a thorough functional and fluid mechanic characterization of the comparatively easily accessible kelp system will help to ask the right questions and identify promising approaches in the experimentally less cooperative tracheophyte systems.

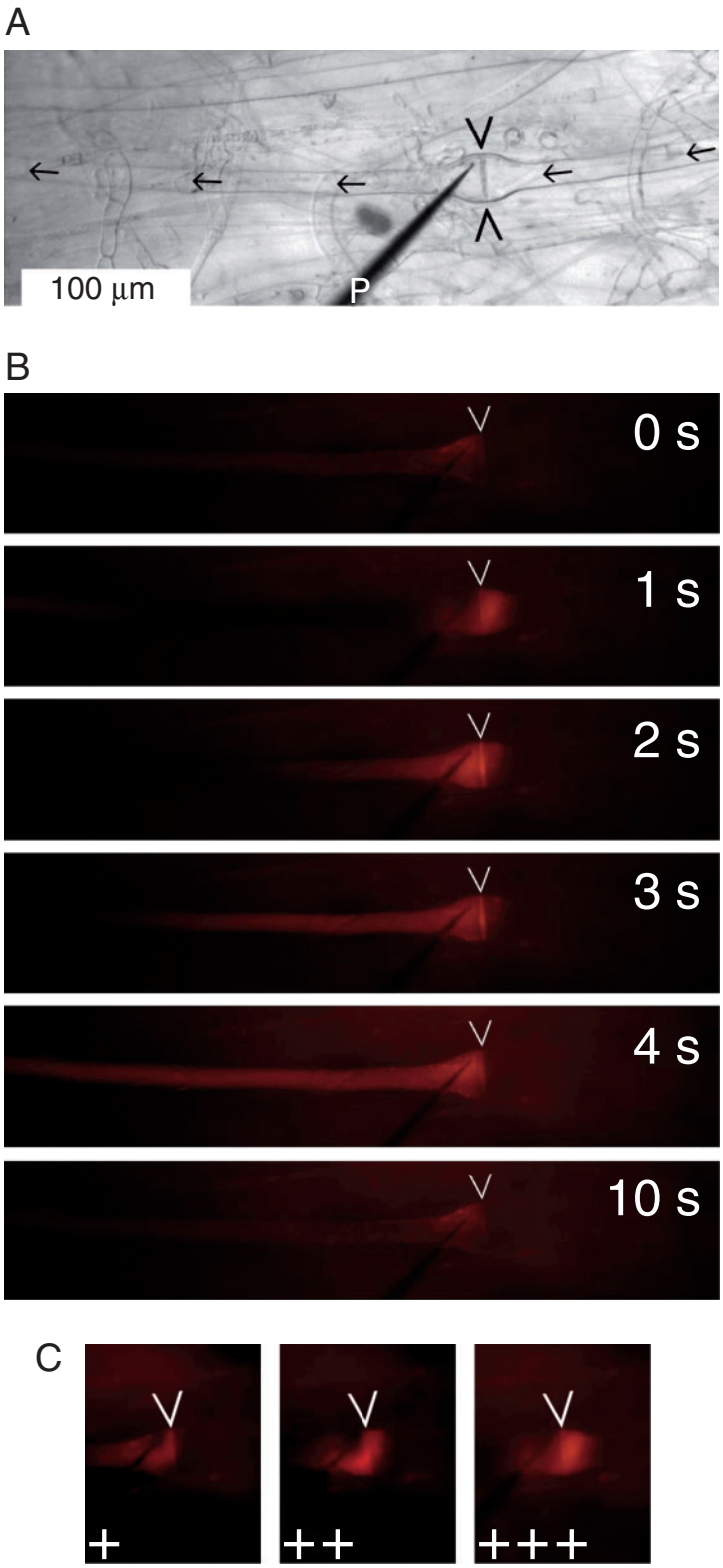

FIG. 4. Pressure-induced reversal of flow direction across a *Nereocystis luetkeana* sieve plate (marked by arrowheads on all micrographs). (A) Brightfield micrograph showing the sieve tube (expected flow direction indicated by arrows) and a micropipette (P) for dye injection placed just downstream of the sieve plate. (B) Fluorescence micrographs of the same sieve tube: time course of dye movement following an injection pulse (1·5 s) starting at 0 s. The injection pressure (IP) drives dye upstream across the sieve plate (1 s) before the dye moves back downstream with the sieve tube flow. (C) Dependence of the maximum extent of upstream dye flow on the IP. Three consecutive injection pulses in the same sieve tube are shown (+, low IP; ++, moderate IP; +++, high IP). The complete experiment is presented as Supplementary Data Video S2.

SUPPLEMENTARY DATA

Supplementary data are available online at www.aob.oxfordjournals.org and consist of the following. Video S1: determination of flow velocity in an individual sieve tube by pulsed injection of a fluorescent dye (rhodamine B). Video S2: transient reversal of flow direction by pressure injection of a fluorescent dye (rhodamine) at the downstream side of a sieve plate; three consecutive injection pulses with increasing injection pressures are shown.

ACKNOWLEDGEMENTS

We acknowledge support by a Herbert L. Eastlick Distinguished Professor Fellowship to M.K. and a sabbatical leave granted to W.S.P. by Indiana/Purdue University Fort Wayne, and thank the Franceschi Microscopy and Imaging Center at Washington State University (Pullman, WA, USA) and Bamfield Marine Research Station (Bamfield, BC, Canada) for logistic support. Constructive criticism by anonymous reviewers helped to improve this manuscript.

LITERATURE CITED

Abadeh A, Lew RR. 2013. Mass flow and velocity profiles in *Neurospora* hyphae: partial plug flow dominates intra-hyphal transport. *Microbiology* **159**: 2386–2394.

Archibald JM. 2012. The evolution of algae by secondary and tertiary endosymbiosis. *Advances in Botanical Research* **64**: 87–118.

Behnke HD, Sjolund RD. 1990. *Sieve elements*. Berlin: Springer.

Buggeln RG. 1983. Photoassimilate translocation in brown algae. *Progress in Phycological Research* **2**: 283–332.

Deniaud-Bouët E, Kervarec N, Michel G, Tonon T, Kloareg B, Hervé C. 2014. Chemical and enzymatic fractionation of cell walls from Fucales: insights into the structure of the extracellular matrix of brown algae. *Annals of Botany* **114**: 1203–1216.

Draget KI, Skjåk-Bræk G, Smidsrød O. 1997. Alginate based new materials. *International Journal of Biological Macromolecules* **21**: 47–55.

Ehlers K, Knoblauch M, van Bel AJE. 2000. Ultrastructural features of well-preserved and injured sieve elements: minute clamps keep the phloem transport conduits free for mass flow. *Protoplasma* **214**: 80–92.

Esau K. 1969. *The phloem*. Berlin: Gebrüder Borntraeger.

Evert RF. 1982. Sieve tube structure in relation to function. *BioScience* **32**: 789–795.

Froelich DR, Mullendore DL, Jensen KH, *et al.* 2011. Phloem ultrastructure and pressure flow: sieve-element-occlusion-related agglomerations do not affect translocation. *The Plant Cell* **23**: 4428–4445.

Fischer A. 1885. Ueber den Inhalt der Siebröhren in der unverletzten Pflanze. *Berichte der Deutschen Botanischen Gesellschaft* **3**: 230–239.

Jensen KH, Mullendore DL, Holbrook NM, Bohr T, Knoblauch M, Bruus H. 2012. Modeling the hydrodynamics of phloem sieve plates. *Frontiers in Plant Science* **3**: 151.

Johnson RPC, Freundlich A, Barclay GF. 1976. Transcellular strands in sieve tubes; what are they? *Journal of Experimental Botany* **27**: 1117–1136.

Kain JM. 1987. Patterns of relative growth in *Nereocystis luetkeana* (Phaeophyta). *Journal of Phycology* **23**: 181–187.

Katz LA. 2012. Origin and diversification of eukaryotes. *Annual Review of Microbiology* **66**: 411–427.

Kloareg B, Quatrano RS. 1988. Structure of the cell walls of marine algae and ecophysiological functions of the matrix polysaccharides. *Oceanography and Marine Biology: Annual Review* **26**: 259–315.

Knoblauch M, van Bel AJE. 1998. Sieve tubes in action. *The Plant Cell* **10**: 35–50.

Knoblauch M, Oparka K. 2012. The structure of the phloem – still more questions than answers. *The Plant Journal* **70**: 147–156.

Knoblauch M, Peters WS. 2010. Münch, morphology, microfluidics – our structural problem with the phloem. *Plant, Cell and Environment* **33**: 1439–1452.

Knoblauch M, Peters WS. 2013. Long-distance translocation of photosynthates: a primer. *Photosynthesis Research* **117**: 189–196.

Knoblauch M, Froelich DR, Pickard WF, Peters WS. 2014. SEORious business: structural proteins in sieve tubes and their involvement in sieve element occlusion. *Journal of Experimental Botany* **65**: 1879–1893.

Lane CE, Archibald JM. 2008. The eukaryotic tree of life: endosymbiosis takes its TOL. *Trends in Ecology and Evolution* **23**: 268–275.

Mullendore DL, Windt CW, van As H, Knoblauch M. 2010. Sieve tube geometry in relation to phloem flow. *The Plant Cell* **22**: 579–593.

Münch E. 1930. *Die Stoffbewegungen in der Pflanze*. Jena: Gustav Fischer.

Nicholson NL. 1970. Field studies on the giant kelp *Nereocystis*. *Journal of Phycology* **6**: 177–182.

Nicholson NL, Briggs WR. 1972. Translocation of photosynthate in the brown alga *Nereocystis*. *American Journal of Botany* **59**: 97–106.

Nicholson NL. 1976. Anatomy of the medulla of *Nereocystis*. *Botanica Marina* **19**: 23–31.

Oltmanns F. 1922. *Morphologie und Biologie der Algen. Zweiter Band: Phaeophyceae – Rhodophyceae*. Jena: Gustav Fischer.

Percival E. 1979. The polysaccharides of green, red and brown seaweeds: their basic structure, biosynthesis and function. *British Phycological Journal* **14**: 103–117.

Percival E, McDowell RH. 1981. Algal walls – composition and biosynthesis. In: W Tanner, GO Aspinell, eds. *Encyclopedia of plant physiology*, **Vol. 13B**. Berlin: Springer, 277–316.

Raven JA. 2003. Long-distance transport in non-vascular plants. *Plant, Cell and Environment* **26**: 73–76.

Savage JA, Clearwater MJ, Haines DF, *et al.* 2015. Allocation, stress tolerance and carbon transport in plants: how does phloem physiology affect plant ecology? *Plant, Cell and Environment* (in press). doi: 10.1111/pce.12602.

Schmitz K. 1990. Algae. In: HD Behnke, RD Sjolund, eds. *Sieve elements*. Berlin: Springer, 1–18.

Schmitz K, Lobban CS. 1976. A survey of translocation in Laminariales (Phaeophyceae). *Marine Biology* **36**: 207–216.

Schmitz K, Srivastata LM. 1974. Fine structure and development of sieve tubes in *Laminaria groenlandica* Rosenv. *Cytobiologie* **10**: 66–87.

Schmitz K, Srivastata LM. 1976. The fine structure of sieve elements of *Nereocystis luetkeana*. *American Journal of Botany* **63**: 679–693.

Spanner DC. 1978. Sieve-plate pores, open or occluded? A critical review. *Plant, Cell and Environment* **1**: 7–20.

Springer YP, Hays CG, Carr MH, Mackey MR. 2010. Toward ecosystem-based management of marine macroalgae – the bull kelp, *Nereocystis luetkeana*. *Oceanography and Marine Biology: Annual Review* **48**: 1–42.

Steinbiß HH, Schmitz K. 1973. CO_2-Fixierung und Stofftransport in benthischen marinen Algen. V. Zur autoradiographischen Lokalisation der Assimilattransportbahnen im Thallus von *Laminaria hyperborea*. *Planta* **112**: 253–263.

Thompson MV. 2006. Phloem: the long and the short of it. *Trends in Plant Science* **11**: 26–32.

Vreeland V, Laetsch, WM. 1989. Identification of associating carbohydrate sequences with labelled oligosaccharides. *Planta* **177**: 423–434.

Weatherley PE, Johnson RPC. 1968. The form and function of the sieve tube: a problem in reconciliation. *International Review of Cytology* **24**: 149–192.